energies

MDPI

*Article*

# Development of a Biomass Gasification Process for the Coproduction of Methanol and Power from Red Sea Microalgae

**Abdulrahman A. Al-Rabiah [1,*], Jiyad N. Al-Dawsari [2], Abdelhamid M. Ajbar [1], Rayan K. Al Darwish [1] and Omar Y. Abdelaziz [3]**

[1] Chemical Engineering Department, College of Engineering, King Saud University, Riyadh 11421, Saudi Arabia
[2] King Abdulaziz City for Science and Technology (KACST), Riyadh 11442, Saudi Arabia
[3] Department of Chemical Engineering, Lund University, 221 00 Lund, Sweden
* Correspondence: arabiah@ksu.edu.sa; Tel.: +966-11-4676844; Fax: +966-11-4678770

**Abstract:** In this study, an algae biomass gasification process using a dual fluidized bed with combined power and methanol cogeneration was developed. The gasification process was modeled using Aspen Plus and validated using experimental data of two microalgae species (*Nannochloropsis oculata* and *Dunaliella salina*) commonly found on the western coast of Saudi Arabia. The impacts of different operating conditions, including the gasifier temperature, steam-to-biomass ratio, and algae-char split ratio, on the compositions of four main gases (CO, $CO_2$, $CH_4$, and $H_2$) were investigated. The results of the parametric studies indicated that the gasification temperature has a significant effect on the composition of the synthesis gas, where 700–850 °C was the ideal operating range for gasification. Altering the ratio of biomass to steam showed a slightly smaller effect on the synthesis gas composition. The char split ratio should be kept below 75% to ensure an adequate heat supply to the process. The proposed process successfully converted 45.7% of the biomass feed to methanol at a production capacity of 290 metric tons per day. On the other hand, 38 MW of electricity capacity was generated in the combined power cycle.

**Keywords:** biomass; microalgae; gasification; fluidized bed; methanol; power; process simulation

check for updates

**Citation:** Al-Rabiah, A.A.; Al-Dawsari, J.N.; Ajbar, A.M.; Al Darwish, R.K.; Abdelaziz, O.Y. Development of a Biomass Gasification Process for the Coproduction of Methanol and Power from Red Sea Microalgae. *Energies* **2022**, *15*, 7890. https://doi.org/10.3390/en15217890

Academic Editors: Ana Ramos, Abel Rouboa and Eliseu Monteiro

Received: 29 September 2022
Accepted: 21 October 2022
Published: 24 October 2022

**Publisher's Note:** MDPI stays neutral with regard to jurisdictional claims in published maps and institutional affiliations.

**Copyright:** © 2022 by the authors. Licensee MDPI, Basel, Switzerland. This article is an open access article distributed under the terms and conditions of the Creative Commons Attribution (CC BY) license (https://creativecommons.org/licenses/by/4.0/).

## 1. Introduction

The petroleum industry has proven to be the primary source providing the world with energy and valuable chemical products for decades. However, the fast growth of the world population and the increase in the use of electrical-driven processes have led to a considerable increase in energy demand, especially in the industrial sector, which is responsible for almost half of the total energy consumption [1]. Traditional fossil fuels are responsible for releasing large quantities of carbon dioxide when burned. Carbon emissions trap heat in the atmosphere and have led to detrimental climate change. Research into renewable energy is actively being pursued to mitigate global climate challenges and preserve sustainability. In this regard, several approaches have been developed to capture carbon dioxide, including absorption and adsorption methods [2]. Another well-known approach is using living organisms in a method known as biocapture, biofixation, or biosequestration [3]. Living organisms such as plants, trees, algae, and microalgae can be used to capture carbon dioxide and can perform photosynthesis processes within their metabolic pathways [4].

Biomass from microalgae has been receiving increasing attention in the scientific literature as a potentially efficient renewable energy source [3–8]. Microalgae are microscopic unicellular plants that can grow in freshwater and marine environments. They are known to grow fast, have smaller land requirements and water consumption compared to conventional land-crop biofuels, and have high photosynthetic efficiency [3–9]. Autotrophic microalgae utilize carbon dioxide to produce hydrogen or carbohydrates, proteins, and

lipids, which can be further used as feedstocks. They can also undergo biochemical conversions in order to obtain bioalcohols, biodiesels, biogas, and biohydrogen. The feedstock may also undergo direct conversion to obtain algal oil, animal food, fish food, and fertilizer. In addition to this, they may also undergo thermochemical conversions to obtain biosynfuels, biodiesel, and biogas [10–17].

Algae utilize $CO_2$ through photosynthesis during their cultivation phase. The biomass feedstock is produced with a high rate of growth and has the ability to grow under unfavorable conditions [5]. Besides their high photosynthetic activity, algae require about 1.8 kg of $CO_2$ per kg of generated biomass [5–9]. The $CO_2$ fixation efficiency for microalgae is about 10–50 times higher than for terrestrial plants, resulting in remarkable 78% and 50% reductions in carbon dioxide and carbon monoxide emissions, respectively [5–9]. The advantages of using microalgae as a feedstock for power generation or biofuel production are numerous [5–9]: (i) flue gases with varying amounts of $CO_2$ can be fed directly to the microalgae culture, greatly simplifying $CO_2$ separation from the flue gas; (ii) certain combustion products, such as $NO_x$ or $SO_x$, can be used effectively as microalgae nutrients; (iii) the microalgae have the potential to yield high-value commercial products that could offset the capital and operating costs of the process; (iv) the sulfur content of the cultivated microalgae biomass is significantly lower than fossil fuels, and thus sources of harmful emissions (e.g., $SO_x$) would be minimized or even eliminated when using algae biomass as a feedstock; (v) microalgae farming does not require freshwater because most of the nutrients required for algae growth are already present in the seawater; and (vi) the process is a truly renewable cycle with minimal environmental impact.

Gasification generally refers to the thermochemical conversion of carbonaceous materials to combustible gases with a usable heating value, mainly containing $H_2$, CO, $CO_2$, and $CH_4$ [12,16,17]. Compared to the incineration and combustion of solid fuel, gasification produces syngas that has less solid waste and emits fewer harmful gases. It is estimated that the use of advanced gasification technology with carbon capture and sequestration (CCS) can store up to 90% of the $CO_2$ released from facilities using conventional fossil fuels and hydrogen [12,16,17]. Talaghat et al. [15], for instance, carried out an experimental study and modeled biodiesel production from two types of microalgae, including *Enteromorpha-compressa and Scenedesmus*, in the presence of an acid catalyst and methanol in batch reactors. The authors showed that more than 99% efficiency could be achieved with optimal conditions. The performance of the gasification process may be affected by different parameters such as the gasifying agents, gasification method, operational conditions, and gasifier type. A fluidized-bed gasifier is known to show high adaptability for syngas production [18]. However, this gasifier has low efficiency, and an external heat source is needed for the endothermic gasification reaction [18]. Alternatively, dual fluidized-bed (DFB) gasification is a new concept that offers a solution to this problem by separating the combustion zone from the gasifier, which provides the necessary energy to the system without the limitations of the gasification agent [16].

Methanol (MeOH) is an important chemical in the industry that can be used as a fuel or a solvent or can be blended with gasoline [19]. MeOH is also utilized to produce a variety of petrochemical products such as methyl tert-butyl ether (MTBE), dimethyl ether (DME), and dimethyl carbonate (DMC) [20,21]. The synthesis gas is used as a feedstock to produce MeOH. The synthesis gas (CO, $CO_2$, or $H_2$) is produced either via steam reforming, dry reforming, or by the gasification process of hydrocarbon or biomass materials [21–23].

Based on the aforementioned literature survey, it can be seen that the algae biomass gasification process was studied using a fluidized-bed technology. The novelty of this paper comprises in three aspects: (1) a novel process for the simultaneous coproduction of biomethanol and electricity is proposed; (2) red sea algae was utilized as a renewable feedstock; and (3) a novel gasification process using Aspen Plus was developed based on the dual fluidized-bed technology.

The performance of the gasification process with respect to the composition of the synthesis gas as well as the effects of microalgae strains, the steam/biomass ratio, and the

char split ratio were investigated. In addition, a parametric study was carried out where key parameters such as the gas temperature and the steam/biomass ratio were varied over large and realistic ranges for the purpose of finding the values of these parameters that would yield the maximum values of syngas ($H_2$ and CO).

## 2. Materials and Methods

### 2.1. Microalgal Biomass Feedstock

Microalgal biomass could be a reliable source of renewable energy and biofuels for industry. Table 1 shows a comparative screening analysis of the biomass and lipid productivity of various microalgae of interest found on Saudi Arabia's eastern and western coastlines [8–12]. Two strains of microalgae (*Nannochloropsis oculata* and *Dunaliella salina*) found in the Red Sea (western coast of Saudi Arabia) were chosen as the feedstock for this study. Table 2 shows the proximate and ultimate analyses of these microalgae. According to this table, the heating value of biomass 2 is high, which is a good feature in power generation systems. However, the ash content is slightly higher, which would increase the sole waste [4,17]. Table 3 summarizes the operating conditions and design parameters of the different microalgal gasification processes found in the literature [3,8,15–18].

**Table 1.** Biomass and lipid productivities of various microalgae found on Saudi Arabia's eastern and western coastlines [8–12].

| Species | Media | Biomass Productivity (g/L/d) | Lipid Productivity (mg/L/d) | Location in Saudi Arabia | Abundance Level |
|---|---|---|---|---|---|
| *Chlorella* | Fresh | 0.23 | 78 | S | Very common |
| *Cylindrotheca* | Marine | 0.43 | 114 | Q + R | Very common |
| *Nannochloropsi* sp. | Marine | 0.21 | 52 | H | Very common |
| *Vulgaris* | Fresh | 0.16 | 30 | D | Rare |
| *Thalassiosira* | Marine | 0.06 | 43 | D + R | Rare |
| *Chlamydomonas* sp. | Fresh | 0.43 | 22 | Q + R | Very common |
| *Dunaliella salina* | Salt | 0.27 | 53 | Q + R | Very common |
| *Oscillatoria* | Fresh | 0.37 | 27 | H | Rare |
| *Nannochloropsis oculata* | Marine | 0.05 | 24 | S + R | Common |
| *Spirulina platensis* | Salt | 0.29 | 75 | Q | Common |
| *Amphora* | Marine | 0.23 | 117 | D | Common |
| *Oscillatoria* | Fresh | 0.37 | 27 | H | Rare |
| *Euglena gracilis* | Fresh | 0.18 | 37 | S | Common |
| *Neochloris oleoabundans* | Fresh | 0.46 | 164 | R | Very rare |

S = Safwa, Q = Al-Qatif, R = Red Sea, H = Saihat, D = Dammam.

**Table 2.** Specification of microalgae used in this study [24,25].

| | Biomass 1 *Nannochloropsis oculata* | Biomass 2 *Dunaliella salina* |
|---|---|---|
| Proximate Analysis (wt% dry) | | |
| Moisture | 6.71 | 4.00 * |
| Ash | 6.4 | 7.2 * |
| Volatiles | 78.94 | 76.3 * |
| Fixed Carbon | 7.95 | 12.3 * |
| Ultimate Analysis (wt% dry) | | |
| Carbon (C) | 47.5 | 48.1 |
| Hydrogen (H) | 6.15 | 7.1 |
| Oxygen (O) | 46.35 | 23.3 |
| Nitrogen (N) | n.a | 9.4 |
| Sulfur (S) | n.a | 0.9 |
| Other properties | | |
| HHV (MJ/kg) | 15.07 | 21.2 |

* Air-dried basis.

**Table 3.** Summary of previous literature on microalgae gasification [10,12,17,26–28].

| | **Aziz et al. (2017)** | **Gaël (2015)** | **Fiori et al. (2012)** | **Adnan et al. (2018)** | **Adnan et al. (2017)** | **Raheem et al. (2017)** |
|---|---|---|---|---|---|---|
| Products | MCH + Electricity | SNG | Hydrogen | Syngas | Syngas | Syngas |
| Feedstock | *Chlorella vulgaris* | *Phaeodactylum tricornutum* | *Spirulina* | *Nannochloropsis oculta* | *Nannochloropsis oculta* | *Chlorella vulgaris* |
| Gasifier type | Fluidized bed | Fixed bed | Fluidized bed | Fluidized bed | Fluidized bed | Fluidized bed |
| Pressure (MPa) | 30 | 30 | 30 | 2-8 | 0.1 | n.r. |
| Temperature (°C) | 600 | 450 | 700 | 700 | 800 | 850 |
| Oxidant | Supercritical water | Supercritical water | Supercritical water | $H_2O/CO_2/O_2$ | $H_2O/O_2$ | Air |
| Catalyst | $Ru/TiO_2$ | Ru/C | n.r. | — | — | — |
| Capture method | Membrane | n.r. | n.r. | n.r. | n.r. | n.r. |
| Gas composition | $H_2$: 46.1%<br>CO: 3.10%<br>$CO_2$: 27.8%<br>$CH_4$: 18.1% | $H_2$: 24.1%<br>CO: 00.0%<br>$CO_2$: 28.9%<br>$CH_4$: 44.8% | $H_2$: 40.1%<br>CO: 05.8%<br>$CO_2$: 32.8%<br>$CH_4$: 25.8% | $H_2$: 31.3%<br>CO: 62.2%<br>$CO_2$: 6.0%<br>$CH_4$: 0.4% | $H_2$: 30.4%<br>CO: 63.2%<br>$CO_2$: 6.04%<br>$CH_4$: 0.38% | $H_2$: 30.7%<br>CO: 24.4%<br>$CO_2$: 27.9%<br>$CH_4$: 19.2% |

MCH = methylcyclohexane. SNG = synthetic natural gas. Syngas = synthetic gas. n.r. = not reported.

### 2.2. Process Concept and Modeling

The proposed block flow diagram of the microalgae gasification plant is shown in Figure 1. This block flow diagram represents a simplified scheme of a general gasification plant with system components for the coproduction of methanol and electricity. The biomass is fed into a dryer unit to remove moisture content (roughly between 30 to 70 wt%). Then, a separation unit is used to separate the steam from the feedstock. The dried feed is then fed to a gasification reactor that operates at 700–800 °C via an airtight closure (except in an open-top gasifier). The processes of pyrolysis, oxidation, and reduction occur in the gasification reactor and its auxiliary reactors.

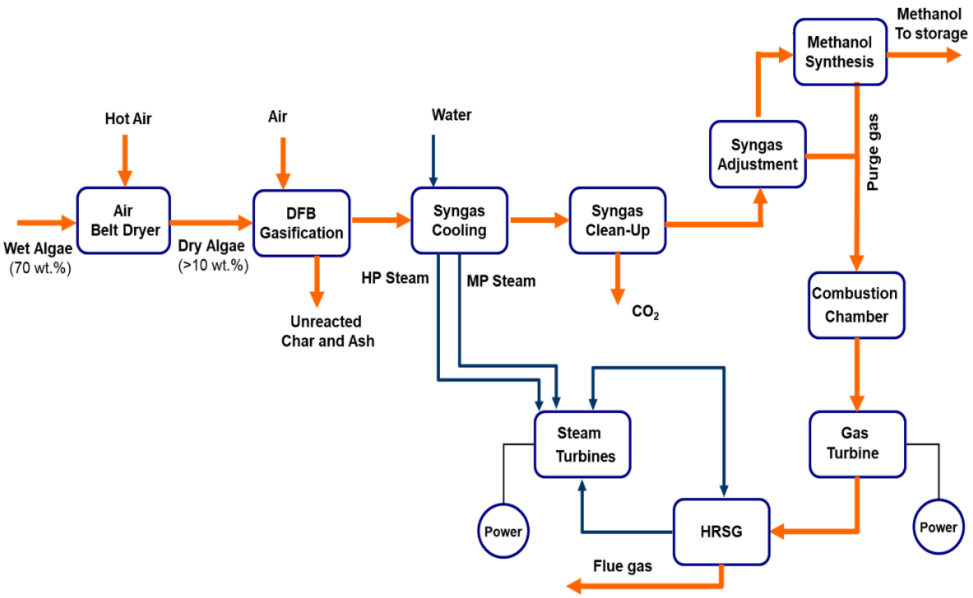



**Figure 1.** Block flow diagram of the integrated gasification combined cycle with methanol synthesis using a dual fluidized-bed gasifier.

A steam-blown dual fluidized-bed gasifier (DFB) was used to separate the gasification and combustion zones in order to avoid nitrogen dilution of the syngas (due to the combustion of fuel with air). Thus, a high-quality gas will be produced without the need for an expensive air separation unit [18]. In this zone, the following set of consecutive reactions were assumed to be the main reactions [16]:

$$\text{Water–gas shift}: \ CO + H_2O \leftrightarrow \ CO_2 + H_2 \qquad \Delta H^o_{298} = -41 \text{ MJ/kmol} \tag{1}$$

$$\text{Methanation}: \qquad C + 2\ H_2 \leftrightarrow \ CH_4 \qquad \Delta H^o_{298} = -75 \text{ MJ/kmol} \tag{2}$$

$$\text{Boudouard}: \qquad C + CO_2 \leftrightarrow \ 2CO \qquad \Delta H^o_{298} = +172 \text{ MJ/kmol} \tag{3}$$

$$\text{Water–gas}: \ C + H_2O \leftrightarrow \ CO + H_2 \qquad \Delta H^o_{298} = +131 \text{ MJ/kmol} \tag{4}$$

$$\text{Steam–methane reforming}: \ CH_4 + H_2O \leftrightarrow \ 3H_2 + CO \ \Delta H^o_{298} = +206 \text{ MJ/kmol} \tag{5}$$

The produced gas leaves the reactor with a particular pollutant, then is subjected to a dry (hot) and/or wet cleaning to satisfy the respective cleanliness requirements for further use in a gas utilization unit (gas engine, gas turbine, microgas turbine, and possibly a fuel cell). The syngas is also conditioned, which typically includes adjusting the $H_2/CO$ ratio by the water–gas shift reaction to optimize the methanol synthesis. For this purpose, the optimal stoichiometric number (SN = $\frac{[H_2]-[CO_2]}{[CO]+[CO_2]}$) should be slightly above two [16,18]. The conditioning of the syngas also typically includes $CO_2$ removal because $CO_2$ slows down the chemical reactions producing methanol and enables the use of smaller downstream equipment [16]. Methanol synthesis is carried out in a catalytic reactor at elevated pressures and temperatures. The reactor product gas is cooled, whereby methanol, condensed to a liquid, is sent to a fractional distillation, where it is separated from water, absorbed gasses, and other byproducts. The syngas not converted to methanol can be used as fuel in a gas turbine or burned to generate electricity.

In this study, a quasi-isothermal Lurgi reactor was simulated for methanol production. A Langmuir–Hinshelwood–Hougen–Watson (LHHW) kinetic model was used, as proposed by Chen for the reaction shown below [29]:

$$\text{Methanol from } CO_2: \ 3H_2 + CO_2 \leftrightarrow \ CH_3OH + H_2O \ \Delta H^o_{298} = -40.9 \ \frac{\text{MJ}}{\text{kmol}} \tag{6}$$

The reaction rate for the first reaction for methanol production from carbon dioxide is given in Equation (7), while the water–gas shift reaction rate is shown in Equation (8). The validated ranges for this kinetic model are 15 to 51 bar and 180 to 280 °C [29–31].

$$r_{methanol} = k_{methanol} \ \frac{\left(P_{CO_2}\ P_{H_2}\right) - \left(1/K_{pmethanol}\right)\left(P_{CH_3OH}P_{H_2O}/P^2_{H2}\right)}{\left(1 + K_a\left(P_{H_2O}/P_{H_2}\right) + K_b\sqrt{P_{H_2}} + K_cP_{H_2O}\right)3} \tag{7}$$

$$r_{WGS} = k_{WGS} \ \frac{P_{CO_2} - \left(1/K_{pWGSl}\right)\left(P_{CO}P_{H_2O}/P_{H_2}\right)}{\left(1 + K_a\left(P_{H_2O}/P_{H_2}\right) + K_b\sqrt{P_{H_2}} + K_cP_{H_2O}\right)} \tag{8}$$

In these equations, *r*i = reaction rate (mol $kg^{-1}_{cat}$ $s^{-1}$), *k*i = kinetic factor (kmol $kg^{-1}_{cat}$ $s^{-1}$ $bar^{-1}$ or kmol $kg^{-1}_{cat}$ $s^{-1}$ $bar^{-2}$), *p*i = partial pressure (bar), $K_{a/b/c}$ = adsorption constants ($bar^n$), and *K*pi = equilibrium constant (- or $bar^{-2}$).

## 3. Results and Discussion

### *3.1. Process Development and Simulation*

The gasifier was simulated based on a dual fluidized-bed gasifier scheme. It was necessary to divide the process into several blocks that could be simulated with the existing models provided by Aspen Plus, as shown in Figure 2. The Peng–Robinson cubic equation of state with the Boston–Mathias alpha function (PK-BM) was selected as the global property method for this model. The PK-BM property method is known to be suitable for gas

processing and petrochemical applications [17]. Table 4 summarizes the assumptions made in formulating the model.

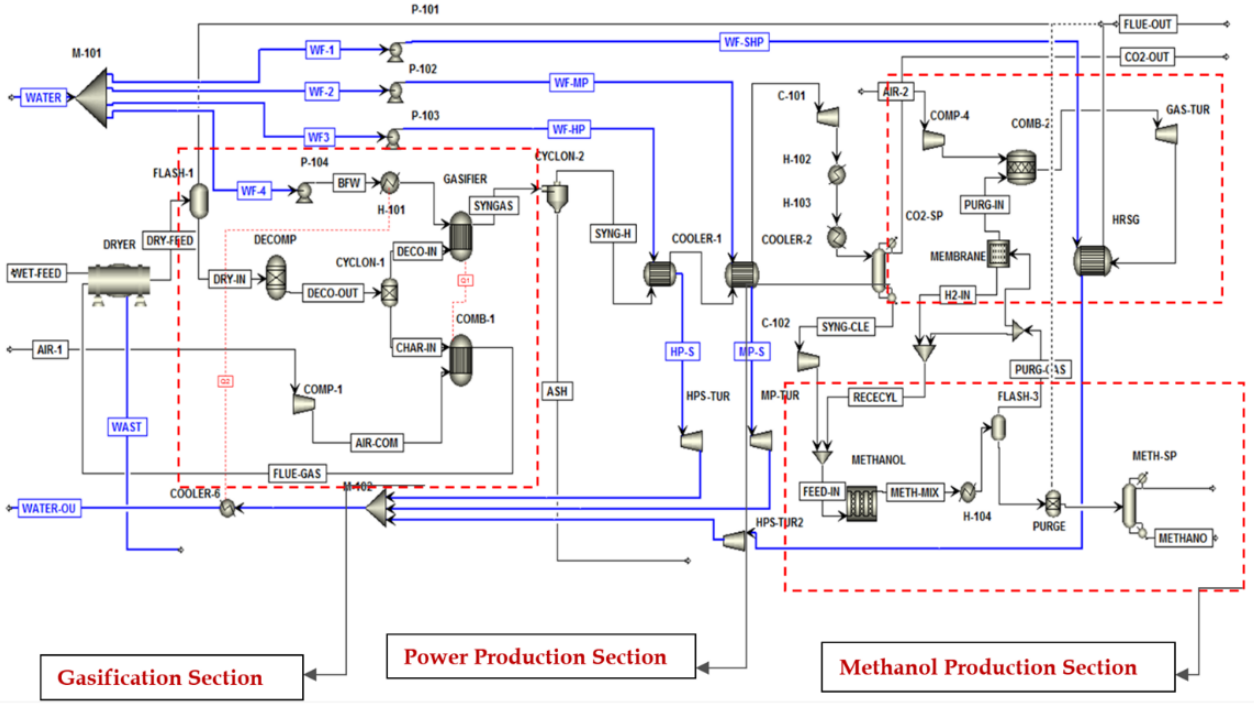



**Figure 2.** Aspen Plus flowsheet simulation of the cogeneration process of methanol and electricity from microalgae biomass.

**Table 4.** Assumptions for the biomass algae feed.

| List of Assumptions |
| --- |
| • Microalgae are made up of carbon, hydrogen, oxygen, and nitrogen. |
| • The main components of volatile products are $H_2$, CO, $CO_2$, and $CH_4$. |
| • The process is isothermal and at a steady state. |
| • $N_2$ is considered inert in the entire process. |
| • Particles are of uniform size and are of spherical shape. |
| • Char only consists of graphitic carbon. |

### 3.1.1. Gasification

A DFB gasifier consists of two fluidized beds: (1) a bubbling fluidized-bed gasifier that converts the feed into raw syngas and (2) a riser section consisting of either a fast fluidized-bed combustor or a circulating fluidized bed that oxidizes the residual char and thus provides heat for the endothermic gasification reactions. The two fluidized beds are interconnected to ensure the circulation of bed material particles. A cyclone separator is used to separate the flue gas and the heat-carrying materials in the riser section. The heat-carrying material is returned to the gasifier while the flue gases go to the heat recovery system. The product gas obtained from the gasifier consists primarily of $H_2$, CO, $CO_2$, and $CH_4$ [32,33].

The process flow diagram (PFD) for the gasification section is shown in Figure 3. The process began by feeding the biomass as a nonconventional component into a dryer (represented by RStoic as an external FORTRAN subroutine). Most of the water content was removed by the dryer and sent to the wastewater treatment. The remaining moister content was removed in the separation unit and discharged with the flue gas. The dried biomass was then fed to a DFB gasifier, represented by three reactors in this simulation. The decomposition stage (represented by RYIELD) converted the biomass into conventional

components by calculating its ultimate and proximate analyses. A routine provided by Aspen Plus was used to determine the yields of the components. The decomposition mixture was then sent to a separator, where a portion of the char was separated and sent to the combustor. The char was combusted (represented by RGIBBS) with excess air, and the generated heat was used to support the endothermic reactions in the gasifier. The gaseous stream and a certain amount of the char were fed to the gasifier. This data block aimed to simulate the reaction between the gasifying agent and the biomass char (Equations (1)–(5)), which were introduced to the reactor at 350 °C. The gasifier effluent of the first stage was sent to a treatment unit in which acidic gases (i.e., $CO_2$) were removed via a physical solvent (represented by the component splitter) and fine particles. The syngas was continuously treated and cleaned from ash and other impurities. The gas cleaning methods that were considered in this study for syngas treatment included particle removal by a filter and a cyclone, and guard beds (ZnO and active carbon filters) to remove trace impurities.

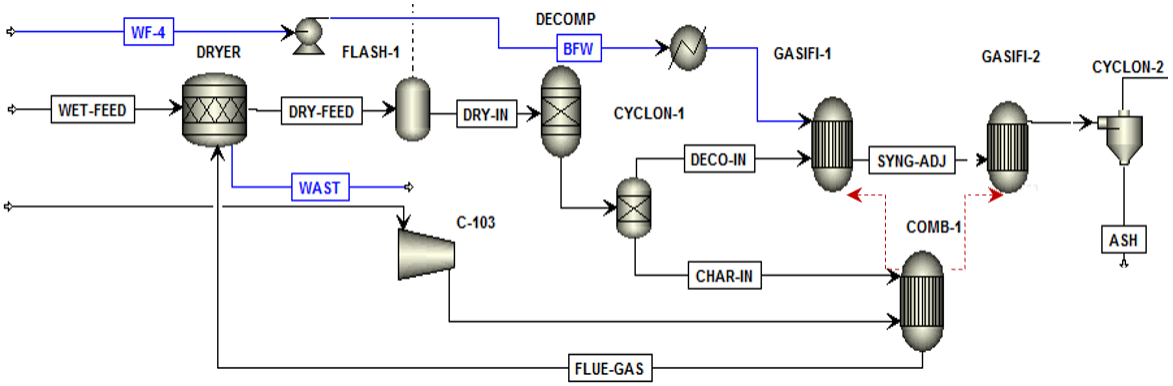



**Figure 3.** Process flow diagram for biomass gasification simulation using Aspen Plus.

### 3.1.2. Power and Methanol Production

In this stage, high-pressure (HP) and medium-pressure (MP) steam were generated from the cooling units used in the steam turbines for power generation. Since the gasification reactor operated at atmospheric pressure, a compressor unit was needed to bring the syngas to the methanol reactor at a high operating pressure. The Plug-Flow Module of Aspen Plus with the LHHW kinetic model was used for modeling the methanol reactor. Two reactions were modeled: methanol formation from $CO_2$ and the RWGS reaction. The primary purpose for such a reactor is that a recycled feed is required to bring the methanol conversion to 50% or 60%. Still, in this case, the recycled feed was introduced with a splitting ratio of 0.5 to 0.6, where the remaining portion was sent to the combustion zone for power production. However, this portion of syngas contained a high amount of $H_2$ gas that needed to be separated before the combustion zone using a membrane, which was then mixed with methanol-recycled feed, as shown in Figure 2. Exhaust gas or flue gas leaving the combustion zone was sent to a gas turbine that would generate most of the power in this process. The fuel gas coming from the gas turbine was still at a high temperature. Thus, a heat recovery steam generator (HRSG) unit was required to bring the flue gas to the stake temperature of 150–250 °C. High-pressure (HP) steam was generated in this unit, which was then used in the HP steam turbine. The stream information of selected streams is given in Table 5.

**Table 5.** Stream information of key streams of the developed coproduction process.

| Stream | WET-FEED | SYNG-H | HP-S | MP-S | FEED-IN | METH-MIX | METHANOL |
|---|---|---|---|---|---|---|---|
| Temperature (°C) | 25 | 800 | 506 | 438 | 114 | 239 | 93 |
| Pressure (kPa) | 105 | 100 | 6000 | 2000 | 4500 | 4500 | 280 |
| Mass vapor fraction | 0 | 1 | 1 | 1 | 0.982 | 1 | 0 |
| Mass liquid fraction | 0 | 0 | 0 | 0 | 0.018 | 0 | 1 |
| Mass solid fraction | 1 | 0 | 0 | 0 | 0 | 0 | 0 |
| **Component flow rates in (kg/h)** | | | | | | | |
| $H_2O$ | 0 | 8422 | 8322 | 10,715 | 8468 | 5961 | 59 |
| $N_2$ | 0 | 2403 | 0 | 0 | 5006 | 5006 | 0 |
| $O_2$ | 0 | 0 | 0 | 0 | 0 | 0 | 0 |
| Algae | 92,000 | 0 | 0 | 0 | 0 | 0 | 0 |
| CO | 0 | 16,413 | 0 | 0 | 17,959 | 2974 | 0 |
| $CO_2$ | 0 | 8769 | 0 | 0 | 12,012 | 18,136 | 0 |
| $H_2$ | 0 | 3037 | 0 | 0 | 19,240 | 17,924 | 0 |
| $CH_4$ | 0 | 50 | 0 | 0 | 104 | 104 | 0 |
| C | 0 | 0 | 0 | 0 | 0 | 0 | 0 |
| Ash | 0 | 0 | 0 | 0 | 0 | 0 | 0 |
| $CH_3OH$ | 0 | 0 | 0 | 0 | 482 | 13,165 | 12,115 |

### *3.2. Model Validation*

The gasification process (gasifier unit) was validated using the same operating conditions as in Duman et al. [32]. The feedstock properties were similar to their studies. The produced gas composition was used for validation, as shown in Table 6. The simulation results agree with the overall findings in [34]. However, this model seems to overestimate CO compared to other gases in the final syngas composition. This is similar to the results that Fernandez-Lopez et al. described in their processes [35]. In addition, the high level of SN produced by the second run was adequate for the case of this study, where a slightly less than 60% removal of $CO_2$ was needed to achieve the required feed composition for the methanol reactor for biomass 2 and a 75% removal was required for biomass 1. Hence, the base case is the Red Sea *Dunaliella salina* (biomass 2).

**Table 6.** Gas composition (%vol., dry basis) of this work.

| Compound | Biomass | Biomass 1 | Biomass 2 |
|---|---|---|---|
| | Duman et al. [34] | This Work | This Work |
| $H_2$ | 55.9% | 50.24% | 44.6% |
| CO | 0.6% | 8.23% | 4.08% |
| $CO_2$ | 34.4% | 30.64% | 25.7% |
| $CH_4$ | 10.9% | 10.89% | 25.5% |
| Tar | 2.5% | n.c. | n.c. |
| SN | 0.61 | 0.50 | 0.63 |

n.c. = not calculated.

### *3.3. Parametric Study*

A sensitivity analysis was carried out for the effect of a number of operating parameters. These include the gasifier temperature, char split ratio, steam/biomass ratio, air flow rate, and split ratio. These parameters can affect all aspects of the process performance indicators, including the syngas yield, the syngas composition, the generated and consumed power in the process, and the methanol production capacity.

#### 3.3.1. Effect of Gasifier Temperature

The temperature of the gasifier was varied from 300 to 900 °C. Figure 4 shows the evolution of the main gases, namely $H_2$, CO, $CO_2$, and $CH_4$, versus the gasification temperature. The production of $H_2$ and CO seemed to increase when the gasification temperature

increased, whereas the yield shifted to high methanation at low temperatures. Hence, operating the gasifier at a high temperature (700–850 °C) is preferred for the synthesis of syngas.

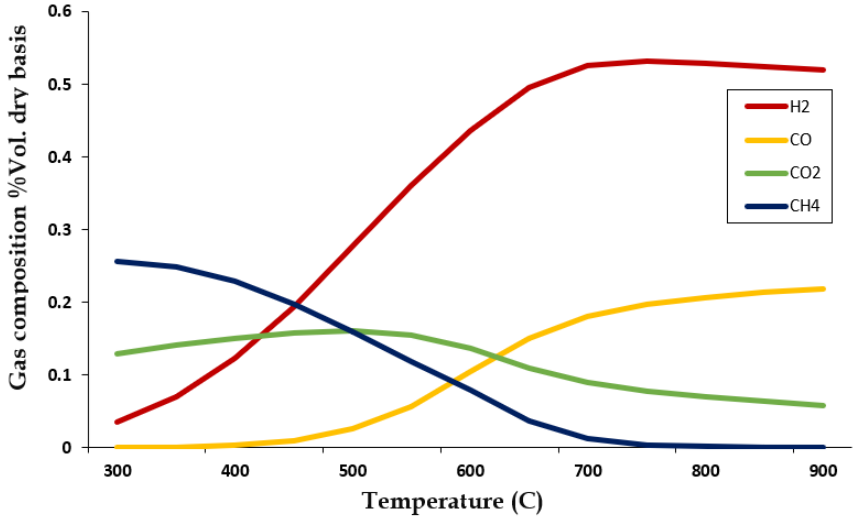



**Figure 4.** Effect of gasifier temperature on the syngas yield.

3.3.2. Effect of the Steam/Biomass Ratio on the Syngas Composition

The gasifying agent/biomass feed ratio was varied from 0.07 to 0.7. The effect of increasing the steam feed in the gasification process is shown in Figure 5. The impact was negative for all gases except $CO_2$, which showed a steady increase in the feed ratio. Hence, operating the gasifier at a lower (i.e., 0.2 to 0.35) steam/biomass ratio produces high-quality syngas.

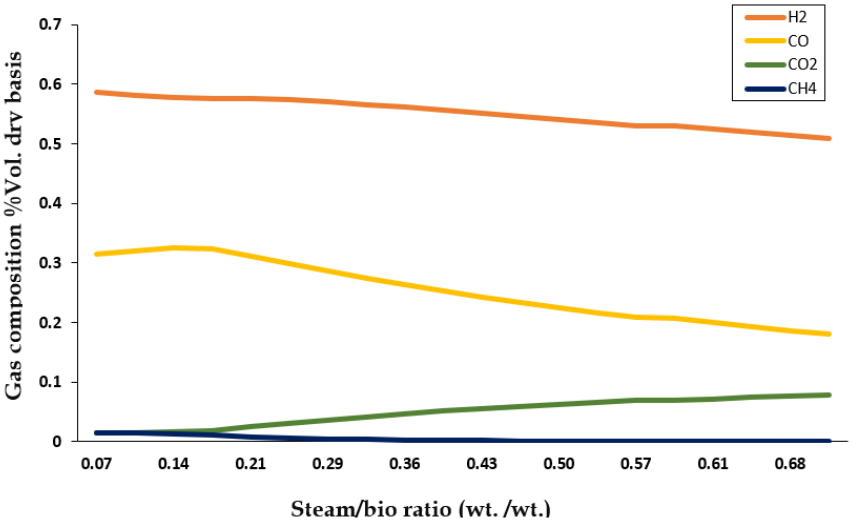



**Figure 5.** Effect steam-to-biomass ratio on the final composition of syngas.

3.3.3. Effect of Char Split Ratio on the Syngas Composition

The split ratio of the char cyclone, a calculator unit of Aspen Plus that represented the splitting of char in the DFB reactor, was varied from 0.5 to 0.9. The effect was minimal on $H_2$, as shown in Figure 6. However, both CO and $CH_4$ seemed to be positively influenced by this increase. The splitting was governed by the amount of heat required in the gasifier. In this work, the splitting ratio was about 20% to 30% to produce the heat required in the gasifier.

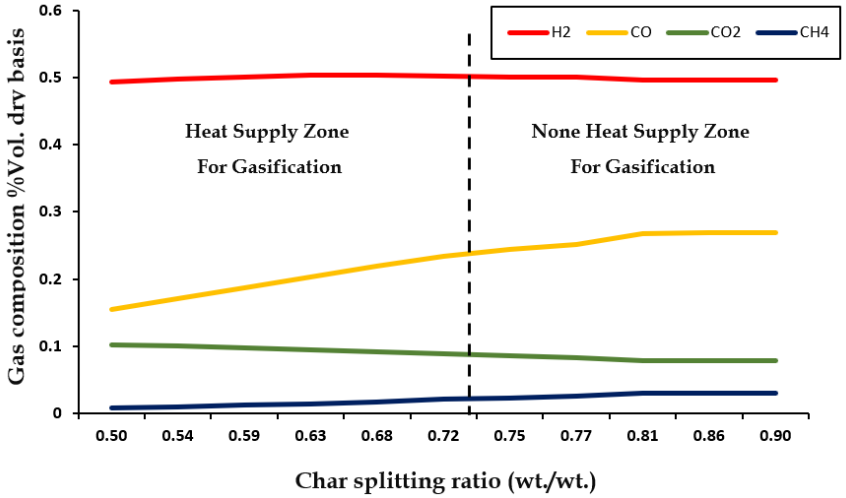



**Figure 6.** Effect of char splitting ratio on the gas yield.

### 3.3.4. Effect of Air Flow Rate on Power Generation

In this analysis, the flow rate of the air that was fed to the combustion zone (COMB-2) was varied from 50.0 to 100.0 tonne/h to study the effect on the power generation by the gas turbine (GAS-TUR) and the hps turbine (HPS-TUR2) as well as the power consumption by the air compressor (COMP-4). Figure 7 shows the power (generated and consumed) as a function of the air flow rate. The increase in the air flow rate had a direct effect on the power consumption by COMP-4. It was also observed that increasing the flow rate of the air resulted in higher power generation from GAS-TUR. However, increasing the flow rate of the air above 63 tonne/h decreased the power generated from HPS-TUR2. This indicates that increasing the air flow rate above this point has no effect on the combustion process, and excess air increases the power consumed by COMP-4 and decreases the power generated by HPS-TUR2. Therefore, the flow rate of the air feed should be around 63 tonne/h.

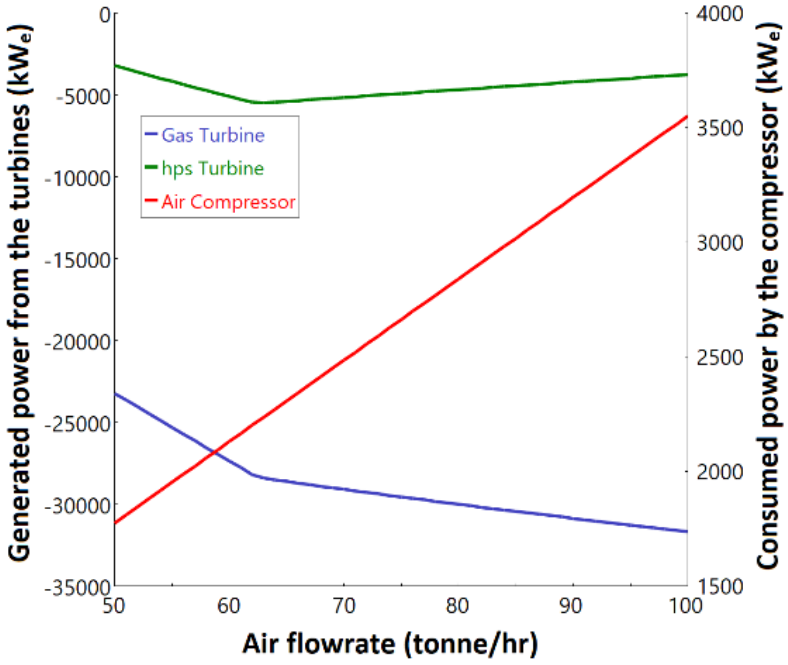



**Figure 7.** Effect of air flow rate on generated and consumed power in the process.

3.3.5. Split Ratio of the Methanol-Recycled Feed

We examined the effect of the split ratio of the methanol-recycled feed, where the ratio varied from 0.4 to 0.6, as shown in Figure 8. The optimal split ratio was selected based on the required production capacity of 100,000 ton per annum of methanol, which was achieved at a split ratio of 0.54. Above this ratio, the methanol capacity increased at the expense of the power cycle unit, as shown in Figure 9. Figure 10 illustrates the distribution of power generation in the process using 0.54 as the split ratio. It was found that the gas turbine was responsible for 80% of the total power generated by the process, with the rest being generated from the steam turbines. Figure 11 shows a comparison of the power produced by the process and the amount of power consumed by the equipment in the process.

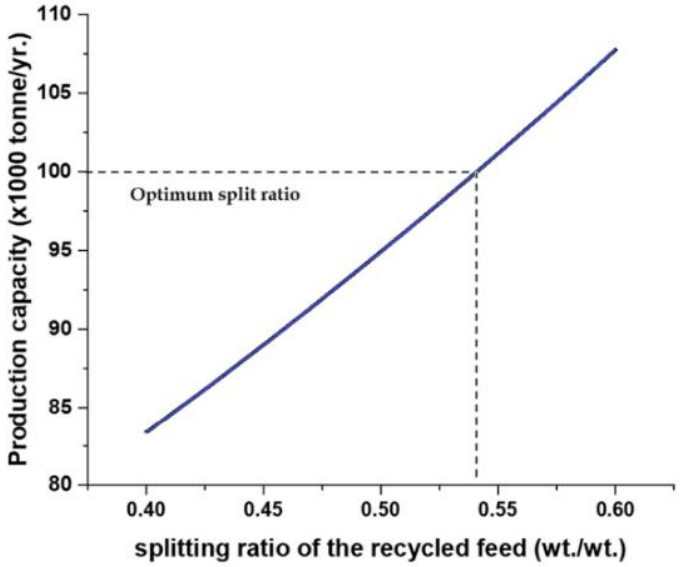



**Figure 8.** Effect of the purge splitting ratio on the methanol production capacity.

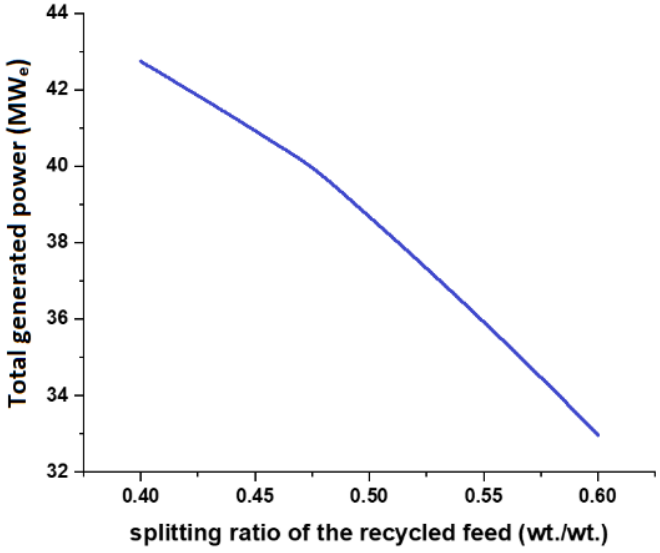



**Figure 9.** Effect of the purge splitting ratio on the produced power.

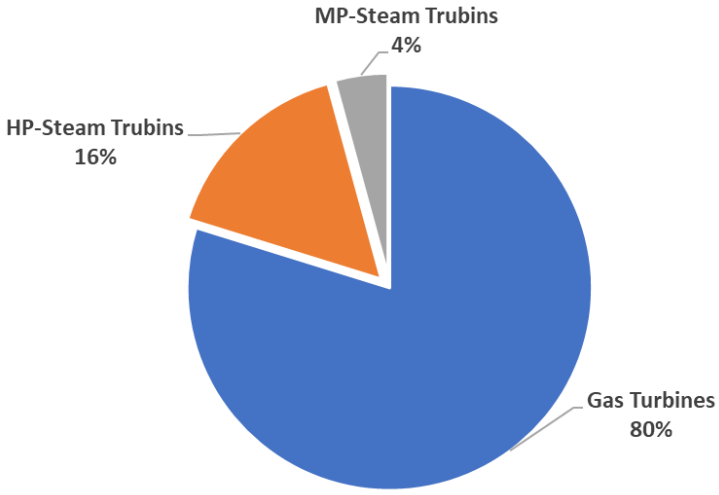



**Figure 10.** Distribution of the power generated by the equipment in the process.

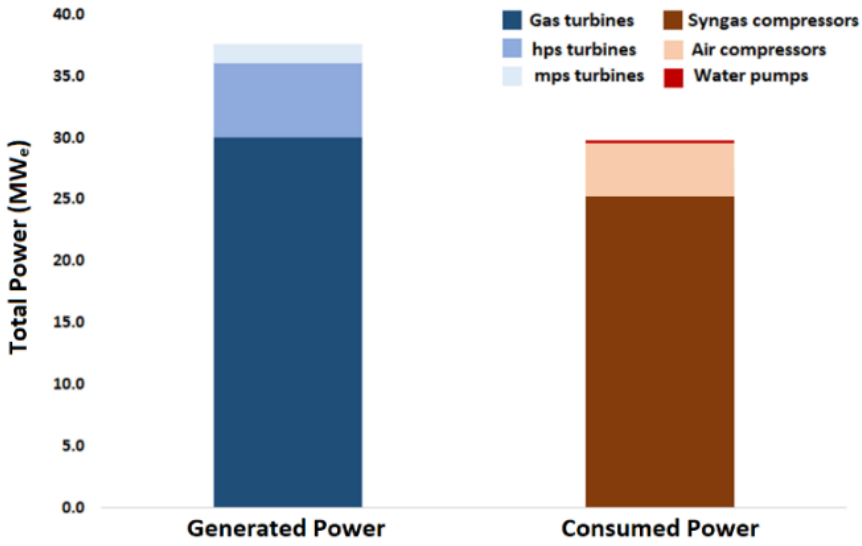



**Figure 11.** Amount of power generated/consumed by the process.

## 4. Conclusions

Algal-based biomass is a promising energy source that is environmentally friendly and carbon neutral. A process for the coproduction of electricity and methanol was developed. The fluidized-bed gasification technology for combined heat and power production using dual fluidized-bed gasification is particularly suitable for biomass utilization. The biomass gasification in a dual fluidized-bed gasifier was simulated using Aspen Plus. The simulation results were validated, and key operating parameters such as the steam-to-biomass ratio, char ratio, and gasification temperature were varied by implementing sensitivity analysis blocks. The effects of these parameters on the syngas composition and the gasification efficiency were studied and outlined. The optimal gasification temperature should be kept around 700–850 °C, while the steam-to-biomass ratio should be kept around 0.4–0.6. If excess heat from the flue gas is available, it should be used to preheat the feed air to the dryer unit. The syngas recycled feed to power generation feed cycle ratio should be around 0.54. This process is advantageous in many respects as it: (i) utilizes multiple gasifying agents without limitation; (ii) utilizes the syngas for various products; (iii) proves to be a self-sustained power process; and (iv) provides high-purity $CO_2$ as the feedstock for algae cultivation farms. Although this research shows promising results, experimental work should be conducted to validate the gasification results for red sea algae. Furthermore, an economic optimization of the process should be carried out in the future.

**Author Contributions:** Conceptualization, A.A.A.-R.; Data curation, A.A.A.-R.; Formal analysis, A.A.A.-R.; Funding acquisition, A.A.A.-R. and O.Y.A.; Investigation, A.A.A.-R. and J.N.A.-D.; Methodology, A.A.A.-R.; Project administration, A.A.A.-R.; Resources, A.A.A.-R.; Software, A.A.A.-R., J.N.A.-D. and R.K.A.D.; Supervision, A.A.A.-R.; Validation, A.A.A.-R., J.N.A.-D., A.M.A., R.K.A.D. and O.Y.A.; Visualization, A.A.A.-R., J.N.A.-D. and R.K.A.D.; Writing—original draft, A.A.A.-R., J.N.A.-D.; Writing—review & editing, A.A.A.-R., A.M.A. and O.Y.A. All authors have read and agreed to the published version of the manuscript.

**Funding:** This study was funded by the Research Center at the College of Engineering, Deanship of Scientific Research, King Saud University.

**Institutional Review Board Statement:** Not applicable.

**Informed Consent Statement:** Not applicable.

**Data Availability Statement:** Not applicable.

**Conflicts of Interest:** The authors declare no conflict of interest.

## References

1. Conti, J.; Holtberg, P.; Diefenderfer, J.; LaRose, A.; Turnure, J.T.; Westfall, L. *USDOE Energy Information Administration (EIA)*; Office of Energy Analysis: Washington, DC, USA, 2016.
2. Jiang, N.; Shen, Y.; Liu, B.; Zhang, D.; Tang, Z.; Li, G.; Fu, B. $CO_2$ capture from dry flue gas by means of VPSA, TSA and TVSA. *J. $CO_2$ Util.* **2020**, *35*, 153–168. [CrossRef]
3. Daneshvar, E.; Wicker, R.J.; Show, P.-L.; Bhatnagar, A. Biologically-mediated carbon capture and utilization by microalgae towards sustainable $CO_2$ biofixation and biomass valorizatio—A review. *Chem. Eng. J.* **2022**, *427*, 130884. [CrossRef]
4. Prasad, R.; Gupta, S.K.; Shabnam, N.; Oliveira, C.Y.B.; Nema, A.K.; Ansari, F.A.; Bux, F. Role of Microalgae in Global $CO_2$ Sequestration: Physiological Mechanism, Recent Development, Challenges, and Future Prospective. *Sustainability* **2021**, *13*, 13061. [CrossRef]
5. Peng, L.; Fu, D.; Chu, H.; Wang, Z.; Qi, H. Biofuel production from microalgae: A review. *Environ. Chem. Lett.* **2020**, *18*, 285–297. [CrossRef]
6. In-na, P.; Umar, A.A.; Wallace, A.D.; Flickinger, M.C.; Caldwell, G.S.; Lee, J.G.M. Loofah-based microalgae and cyanobacteria biocomposites for intensifying carbon dioxide capture. *J. $CO_2$ Util.* **2020**, *42*, 101348. [CrossRef]
7. Rodas-Zuluaga, L.I.; Castañeda-Hernández, L.; Castillo-Vacas, E.I.; Gradiz-Menjivar, A.; López-Pacheco, I.Y.; Castillo-Zacarías, C.; Boully, L.; Iqbal, H.M.; Parra-Saldívar, R. Bio-capture and influence of $CO_2$ on the growth rate and biomass composition of the microalgae *Botryococcus braunii* and *Scenedesmus* sp. *J. $CO_2$ Util.* **2021**, *43*, 101371. [CrossRef]
8. Fantini, M. Biomass availability, potential and characteristics. In *Biorefineries*; Springer: Berlin/Heidelberg, Germany, 2017; pp. 21–54.
9. Yoo, C.; Jun, S.-Y.; Lee, J.-Y.; Ahn, C.-Y.; Oh, H.-M. Selection of microalgae for lipid production under high levels carbon dioxide. *Bioresour. Technol.* **2010**, *101*, S71–S74. [CrossRef]
10. Aziz, M. Integrated hydrogen production and power generation from microalgae. *Int. J. Hydrogen Energy* **2016**, *41*, 104–112. [CrossRef]
11. Bhola, V.; Swalaha, F.; Ranjith Kumar, R.; Singh, M.; Bux, F. Overview of the potential of microalgae for $CO_2$ sequestration. *Int. J. Environ. Sci. Technol.* **2014**, *11*, 2103–2118. [CrossRef]
12. Adnan, M.A.; Hossain, M.M. Gasification performance of various microalgae biomass—A thermodynamic study by considering tar formation using Aspen plus. *Energy Convers. Manag.* **2018**, *165*, 783–793. [CrossRef]
13. Parvez, A.M.; Afzal, M.T.; Hebb, T.G.V.; Schmid, M. Utilization of $CO_2$ in thermochemical conversion of biomass for enhanced product properties: A review. *J. $CO_2$ Util.* **2020**, *40*, 101217. [CrossRef]
14. Bortoleto, G.G.; de Miranda, H.L.; de Campos, R.H. Biodiesel from Microalgae: Third Generation Biofuel. In *Plant-Based Genetic Tools Biofuels Production*; Bentham Science Publishers: Sharja, United Arab Emirates, 2017; pp. 169–198.
15. Talaghat, M.R.; Mokhtari, S.; Saadat, M. Modeling and optimization of biodiesel production from microalgae in a batch reactor. *Fuel* **2020**, *280*, 118578. [CrossRef]
16. Ahmad, A.A.; Zawawi, N.A.; Kasim, F.H.; Inayat, A.; Khasri, A. Assessing the gasification performance of biomass: A review on biomass gasification process conditions, optimization and economic evaluation. *Renew. Sustain. Energy Rev.* **2016**, *53*, 1333–1347. [CrossRef]
17. Fiori, L.; Valbusa, M.; Castello, D. Supercritical water gasification of biomass for $H_2$ production: Process design. *Bioresour. Technol.* **2012**, *121*, 139–147. [CrossRef]
18. Motta, I.L.; Miranda, N.T.; Maciel Filho, R.; Maciel, M.R.W. Biomass gasification in fluidized beds: A review of biomass moisture content and operating pressure effects. *Renew. Sustain. Energy Rev.* **2018**, *94*, 998–1023. [CrossRef]
19. Abdelaziz, O.Y.; Hosny, W.M.; Gadalla, M.A.; Ashour, F.H.; Ashour, I.A.; Hulteberg, C.P. Novel process technologies for conversion of carbon dioxide from industrial flue gas streams into methanol. *J. $CO_2$ Util.* **2017**, *21*, 52–63. [CrossRef]

20. Al-Rabiah, A.A.; Alshehri, A.S.; Ibn Idriss, A.; Abdelaziz, O.Y. Comparative Kinetic Analysis and Process Optimization for the Production of Dimethyl Ether via Methanol Dehydration over a γ-Alumina Catalyst. *Chem. Eng. Technol.* **2022**, *45*, 319–328. [CrossRef]
21. Abashar, M.E.E.; Al-Rabiah, A.A. Highly efficient $CO_2$ hydrogenation to methanol via in-situ condensation and sorption in a novel multi-stage circulating fast fluidized bed reactor. *Chem. Eng. J.* **2022**, *439*, 135628. [CrossRef]
22. Abashar, M.E.E.; Al-Rabiah, A.A. Investigation of the efficiency of sorption-enhanced methanol synthesis process in circulating fast fluidized bed reactors. *Fuel Process. Technol.* **2018**, *179*, 387–398. [CrossRef]
23. Ali, D.A.; Gadalla, M.A.; Abdelaziz, O.Y.; Hulteberg, C.P.; Ashour, F.H. Co-gasification of coal and biomass wastes in an entrained flow gasifier: Modelling, simulation and integration opportunities. *J. Nat. Gas Sci. Eng.* **2017**, *37*, 126–137. [CrossRef]
24. Gong, X.; Zhang, B.; Zhang, Y.; Huang, Y.; Xu, M. Investigation on pyrolysis of low lipid microalgae Chlorella vulgaris and Dunaliella salina. *Energy Fuels* **2014**, *28*, 95–103. [CrossRef]
25. Adnan, M.A.; Hossain, M.M. $CO_2$ gasification of microalgae (N. Oculata)—A thermodynamic study. *MATEC Web Conf.* **2018**, *154*, 1002. [CrossRef]
26. Peng, G. Methane Production from Microalgae via Continuous Catalytic Supercritical Water Gasification: Development of Catalysts and Sulfur Removal Techniques. Ph.D. Thesis, EPFL, Lausanne, Switzerland, 2015.
27. Adnan, M.A.; Susanto, H.; Binous, H.; Muraza, O.; Hossain, M.M. Feed compositions and gasification potential of several biomasses including a microalgae: A thermodynamic modeling approach. *Int. J. Hydrogen Energy* **2017**, *42*, 17009–17019. [CrossRef]
28. Raheem, A.; Dupont, V.; Channa, A.Q.; Zhao, X.; Vuppaladadiyam, A.K.; Taufiq-Yap, Y.-H.; Zhao, M.; Harun, R. Parametric characterization of air gasification of Chlorella vulgaris biomass. *Energy Fuels* **2017**, *31*, 2959–2969. [CrossRef]
29. Chen, L.; Jiang, Q.; Song, Z.; Posarac, D. Optimization of Methanol Yield from a Lurgi Reactor. *Chem. Eng. Technol.* **2011**, *34*, 817–822. [CrossRef]
30. Nestler, F.; Schütze, A.R.; Ouda, M.; Hadrich, M.J.; Schaadt, A.; Bajohr, S.; Kolb, T. Kinetic modelling of methanol synthesis over commercial catalysts: A critical assessment. *Chem. Eng. J.* **2020**, *394*, 124881. [CrossRef]
31. Graaf, G.H.; Stamhuis, E.J.; Beenackers, A.A.C.M. Kinetics of low-pressure methanol synthesis. *Chem. Eng. Sci.* **1988**, *43*, 3185–3195. [CrossRef]
32. Hanchate, N.; Ramani, S.; Mathpati, C.S.; Dalvi, V.H. Biomass gasification using dual fluidized bed gasification systems: A review. *J. Clean. Prod.* **2021**, *280*, 123148. [CrossRef]
33. Thunman, H.; Seemann, M.; Berdugo Vilches, T.; Maric, J.; Pallares, D.; Ström, H.; Berndes, G.; Knutsson, P.; Larsson, A.; Breitholtz, C.; et al. Advanced biofuel production via gasification—Lessons learned from 200 man-years of research activity with Chalmers' research gasifier and the GoBiGas demonstration plant. *Energy Sci. Eng.* **2018**, *6*, 6–34. [CrossRef]
34. Duman, G.; Uddin, M.A.; Yanik, J. Hydrogen production from algal biomass via steam gasification. *Bioresour. Technol.* **2014**, *166*, 24–30. [CrossRef]
35. Fernandez-Lopez, M.; Pedroche, J.; Valverde, J.L.; Sánchez-Silva, L. Simulation of the gasification of animal wastes in a dual gasifier using Aspen Plus®. *Energy Convers. Manag.* **2017**, *140*, 211–217. [CrossRef]